18.7% efficient laser-doped solar cell on *p*-type Czochralski silicon

Z. Hameiri,[a] L. Mai, A. Sproul, and S. R. Wenham
ARC Photovoltaics Centre of Excellence, University of New South Wales, Sydney, New South Wales 2052, Australia

(Received 27 September 2010; accepted 21 October 2010; published online 1 December 2010)

The use of laser doping in solar cell fabrication has received increased attention in recent years, especially due to its ability to form a selective emitter without subjecting the wafer to prolonged high-temperature processes. At the University of New South Wales, a laser doping method was developed that combines the formation of the selective emitter with a self-aligned metallization pattern. This letter reports 18.7% efficient laser-doped solar cells, fabricated on large area commercial-grade *p*-type Czochralski silicon, and analyzes the loss mechanisms. © *2010 American Institute of Physics*. [doi:10.1063/1.3515866]

Laser doping has been employed for more than four decades in semiconductor manufacturing.[1] It was adopted to solar cell fabrication at the beginning of the 1980s (Ref. 2) with increased attention in the past 15 years.[3] The main advantage of this technique is the localized nature of the laser beam, which allows melting of the surface without heating of the bulk, therefore minimizing the degradation associated with high-temperature processes. Other advantages include easy control of doping level and diffusion depth, versatile application, and simple implementation in both laboratory and industrial environments.

At the University of New South Wales (UNSW), a laser doping method has been developed for creating selective emitters.[4] In this method, the dopant source (spin on dopant) is applied onto the dielectric film, which is employed not only as an antireflection coating (ARC) and passivation layer for the surface, but also as a mask for the subsequent metallization process. A laser beam scanning over the areas where metallization will be applied locally melts the silicon, removes the dielectric film, exposes the silicon, and induces diffusion of dopants in the liquid phase. In this way, a selective emitter and self-aligned metallization pattern are formed simultaneously. High efficiency solar cells, both on *n*- and *p*-type substrates, were achieved by this technique.[5,6] After describing the fabrication process, this letter reports the latest results for this solar cell structure on *p*-type silicon and analyses the cells' performance losses.

Large area (154 cm^2) commercial-grade *p*-type Czochralski (CZ) substrates (2 Ω cm) were used to fabricate a batch of ten single-sided laser-doped (SSLD) solar cells. After alkaline texturing and subsequent cleaning, a 40 $\Omega/\square$ emitter was formed in a conventional diffusion tube furnace. Phosphosilicate glass (PSG) removal and edge isolation increased the emitter sheet resistivity value to 75–80 $\Omega/\square$. After a short dry oxidation, an ARC silicon nitride (SiN_x) was deposited using an industrial remote plasma-enhanced chemical vapor deposition (PECVD) system from Roth & Rau. The rear contact was formed by firing screen-printed aluminum paste prior to the laser doping process. The laser-doped areas were formed using a diode-pumped, Q-switched, frequency-doubled $Nd:YVO_4$ laser ($\lambda = 532$ nm) with a Gaussian beam. The melted region was found to be ~ 1 μm deep. Finally, nickel and copper photoplating[7] were performed to form the front contact grid. Table I summarizes the batch average and best solar cell electrical parameters.

Figure 1 presents the current-voltage characteristics of the best solar cell fabricated in this work. An efficiency of 18.7% was achieved on a large area commercial-grade *p*-type CZ substrate. This is believed to be the highest efficiency ever reported for a laser-doped solar cell using commercial-grade wafers.

Figure 2 presents the internal quantum efficiency (IQE) of this solar cell together with modeled data derived from the semiconductor simulation program PC1D.[8] As can be seen, the cell's response to short wavelengths is lower than unity and indicates losses in both the short-circuit current density (J_{sc}) and the open-circuit voltage (V_{oc}) of the device. The relatively low emitter sheet resistivity and the high front surface recombination velocity (SRV) both contribute to this loss. However, increasing the emitter sheet resistivity reduces the fill factor (FF).

In order to identify the optimum emitter sheet resistivity, the PC1D modeling was employed, varying only the emitter resistivity and the front SRV, to obtain the modified J_{sc} and V_{oc}. The variation in the FF was estimated using the expression for the normalized power loss P_{em} due to emitter resistivity given by[9]

$$P_{em} = \frac{\rho_s}{12}\frac{J_{mp}}{V_{mp}}S^2, \tag{1}$$

where J_{mp} and V_{mp} are the current and the voltage at the maximum power point, ρ_s is the emitter sheet resistivity, and S is the spacing between the metal fingers. It was found that a maximum efficiency is achieved for cells with a 120–140 $\Omega/\square$ emitter. The inset in Fig. 2 compares the IQE of a 75 $\Omega/\square$ and 120 $\Omega/\square$ SSLD solar cell, as obtained from the PC1D simulation. The superiority of the

TABLE I. Average and best electrical parameters under standard test conditions (AM 1.5 G spectrum, 100 mW/cm^2, 25 °C).

	V_{oc} (mV)	J_{sc} (mA/cm^2)	FF (%)	Efficiency (%)
Average	629.4	38.0	77.7	18.6
Best cell	632.0	38.0	78.0	18.7

[a]Electronic mail: ziv.hameiri@gmail.com.

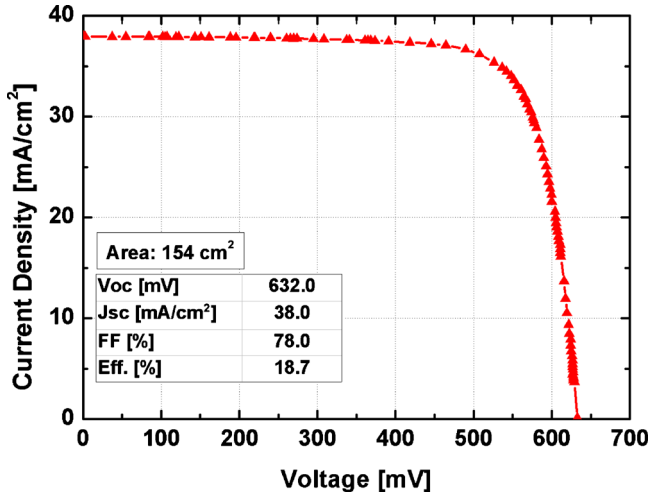

FIG. 1. (Color online) Current-voltage characteristics of the 18.7% efficient laser-doped solar cell (AM 1.5 G, 100 mW/cm^2, 25 °C).

120 Ω/□ emitter cell is demonstrated by the unity spectral response at short wavelengths.

Table II compares the electrical parameters of the SSLD solar cell, its modeled values, and the predicted parameters of a 120 Ω/□ emitter cell. Note that for the 120 Ω/□ cell, a front SRV of 200 cm/s was assumed. A 0.3% absolute increase in the solar cell efficiency is predicted for a modified emitter mainly due to enhancement in the V_{oc}. It was found that reducing the front SRV without increasing the emitter resistivity has a limited impact.

It seems that some manufacturers who fabricate selective-emitter solar cells prefer slightly heavier-doped emitters (<90 Ω/□) under the assumption that absorption in the ethylene vinyl acetate (EVA)—used for encapsulation of cells in standard modules—negates any improvement in device spectral response at short wavelengths.[10] Under these conditions, low emitter sheet resistivity seems beneficial due to reduced resistive loss. However, the PC1D simulation predicts only a small degradation of the FF (−0.5%), smaller than the enhancement of the V_{oc} (+1.6%). Hence, increasing the emitter resistivity to the range of 120 Ω/□ enhances the solar cell efficiency, even without improvement of the current. The development of an EVA with lower absorption will improve solar cell efficiency even further.

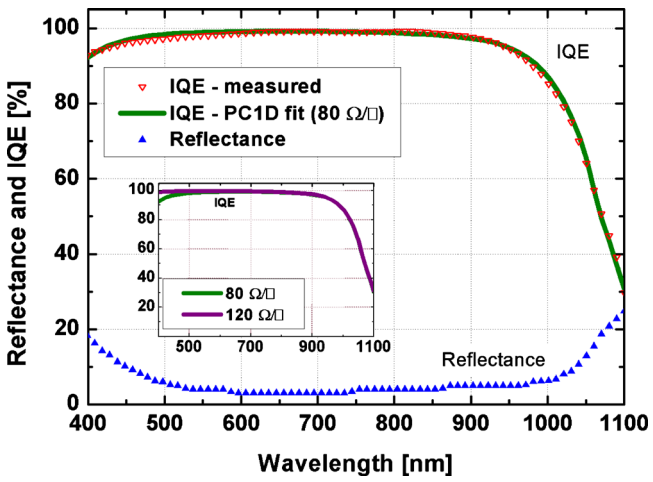

FIG. 2. (Color online) Measured IQE and reflectance curves of 18.7% efficient SSLD. The solid line is the PC1D fit.

TABLE II. Electrical parameters of the 18.7% SSLD solar cell together with the parameters obtained from the PC1D fit. The predicted parameters of a SSLD solar cell with lighter emitter (120 Ω/□) are given as well.

	Measured	PC1D (80 Ω/□)	PC1D (120 Ω/□)
J_{sc} (mA/cm^2)	38.0	37.9	38.3
V_{oc} (mV)	632.0	630.8	640.7
FF (%)	78.0	78.0	77.6
Efficiency (%)	18.7	18.6	19.0

To gain better insight into the recombination losses, the contribution of each fabrication step to the total dark saturation current was investigated. The following experiments utilized the same commercial-grade CZ *p*-type substrates. In order to estimate the wafer quality, two wafers were saw damage etched and cleaned before SiN_x deposition onto both surfaces. A silicon-rich SiN_x film was chosen due to its high quality of passivation.[11] Surface recombination velocity of ~10 cm/s was measured on FZ wafers which were fabricated in conjunction with the CZ substrates. The effective lifetime and the implied V_{oc} were measured using a photoconductance lifetime tester system under quasi steady-state conditions (QSS-PC).[12] The dark saturation current density (J_0) associated with the implied V_{oc} was calculated using

$$J_0 = \frac{J_{sc}}{\exp\left(\frac{V_{oc}}{kT/q}\right)}. \quad (2)$$

A second sample was used to calculate the J_0 associated with the front surface after an emitter diffusion and subsequent processing. After alkaline texturing and subsequent cleaning, a 40 Ω/□ emitter was diffused using a conventional tube furnace. PSG removal and edge isolation increased the emitter sheet resistivity to 80 Ω/□. After a short dry oxidation, an ARC SiN_x was deposited onto the front surface using the industrial remote PECVD system, while a silicon-rich SiN_x film (identical to that used previously) was deposited onto the rear surface as passivation layer. After implied V_{oc} measurements, the total J_0 was calculated using Eq. (2), while the J_0 associated with the front surface was found as the difference between the total J_0 values (total J_0 after this stage and J_0 of the well passivated undiffused wafers—see Table III). The contribution of the emitter and the texturing to the total J_0 and to the reduction in the implied V_{oc} were calculated using PC1D.

A third experiment was carried out to determine the contribution of the rear silicon-aluminum interface to J_0. To do this, the silicon-rich film was removed from the rear surface and was replaced by screen-printed aluminum. The V_{oc} of the device was then measured using a multimeter under one-sun conditions after firing of the aluminum and was then remeasured after the formation of a selective emitter by laser doping. Finally, nickel and copper photoplating were used to form the front grid and contact pads. The nickel sintering was performed at 400 °C using an open air belt furnace. The V_{oc} of the finished solar cells was measured under one-sun illumination. Table III summarizes the V_{oc} and J_0 values after each fabrication step and the contribution of each step to the

TABLE III. Calculated J_0 of different fabrication steps.

Process	V_{oc}/implied V_{oc} (mV)	Total J_0 (A/cm^2)	J_0 of the process (A/cm^2)	Percentage of total J_0
Wafer	688.4[a]	4.2×10^{-14}	4.2×10^{-14}	8
Texturing and emitter	666.3[b]	1.0×10^{-13}	5.9×10^{-14}	11
SiO_2/SiN_x passivation	653.7[a]	1.7×10^{-13}	6.6×10^{-14}	13
Rear contact	628.6	4.6×10^{-13}	2.9×10^{-13}	56
Front laser doping	624.6	5.4×10^{-13}	7.9×10^{-14}	
Metallization	625.5	5.2×10^{-13}	-1.9×10^{-14}	12[c]

[a]Implied V_{oc}.
[b]PC1D calculation.
[c]For both laser doping and metallization.

total J_0. Note that the calculation of J_0 using Eq. (2) is carried out under the assumption that J_{01} (ideality factor of unity) is the dominant recombination process for measurements above. This assumption is reasonably accurate due to the small percentage of laser-doped regions, which contribute also to J_{02}.

It can be seen that the rear surface contributes more than 50% of the total dark saturation current of the finished solar cell. A similar rear side contribution was calculated for the buried-contact solar cell fabricated on a similar 1 Ω cm *p*-type CZ substrate by Wenham.[13] The postmetallization improvement is explained by an improved front surface and bulk passivation due to hydrogenation. Furthermore, the heavy doping beneath the metal isolates this high recombination interface from the active area of the cell, thus minimizing its influence. The results emphasize the importance of high quality rear passivation in order to boost the electrical performance of these cells.

In conclusion, SSLD solar cells with efficiency as high as 18.7% were demonstrated on a large area commercial-grade *p*-type CZ substrate. Two main loss mechanisms were identified. The first one is the relatively heavy-diffused emitter and the corresponding poor front surface passivation. Both were found to degrade the efficiency by absolute 0.3%–0.4%. The second loss mechanism is the rear surface design, as indicated by its contribution to the total dark saturation current. Reducing the rear surface recombination is believed to be the key to achieve efficiencies above 20%.

The ARC Photovoltaics Centre of Excellence is supported by the Australian Research Council under the ARC Centres of Excellence program and the NSW State Government through DSRD. The support of our industry collaborators is also greatly acknowledged.

[1]J. Fairfield and G. H. Schwuttke, Solid-State Electron. **11**, 1175 (1968).
[2]R. T. Young, R. F. Wood, J. Narayan, C. W. White, and W. H. Christie, IEEE Trans. Electron Devices **27**, 807 (1980).
[3]L. Pirozzi, U. Vetrella, and E. Salza, presented at the Laser Applications in Microelectronic and Optoelectronic Manufacturing II, San Jose, CA, 1997, pp. 119–128.
[4]S. R. Wenham and M. A. Green, U.S. Patent No. 6,429,037 (2002).
[5]B. S. Tjahjono, J. H. Guo, Z. Hameiri, L. Mai, A. Sugianto, S. Wang, and S. R. Wenham, presented at the 22nd European Photovoltaic Solar Energy Conference, Milan, Italy, 2007.
[6]L. Mai, Z. Hameiri, B. S. Tjahjono, S. R. Wenham, A. Sugianto, and M. B. Edwards, presented at the 34th IEEE Photovoltaic Specialists Conference (PVSC), 2009, pp. 1811–1815.
[7]S. Morishita, U.S. Patent No. 5,424,252 (1995).
[8]P. A. Basore, IEEE Trans. Electron Devices **37**, 337 (1990).
[9]M. A. Green, *Solar Cells: Operating Principles, Technology and System Application* (University of New South Wales, Sydney, Australia, 1998).
[10]J. Ji (personal communication), 2010.
[11]Z. Hameiri, L. Mai, N. Borojevic, S. Javid, B. Tjahjono, S. Wang, A. Sproul, and S. Wenham, presented at the 34th IEEE Photovoltaic Specialists Conference (PVSC), 2009, pp. 1795–1800.
[12]R. A. Sinton and A. Cuevas, presented at the 16th European Photovoltaic Solar Energy Conference, Glasgow, UK, 2000.
[13]S. Wenham, Prog. Photovoltaics **1**, 3 (1993).